Progress in Organic Coatings 75 (2012) 356–363

Contents lists available at SciVerse ScienceDirect

Progress in Organic Coatings

journal homepage: www.elsevier.com/locate/porgcoat

Synthesis and characterization of epoxy–silicone–polythiophene interpenetrating polymer network for corrosion protection of steel

S. Palraj[a,*], M. Selvaraj[a], M. Vidhya[b], G. Rajagopal[a]

[a] *Central Electrochemical Research Institute, Karaikudi 630 006, Tamil Nadu, India*
[b] *P.S.G.R Krishnammal College for Women, Coimbatore, Tamil Nadu, India*

A R T I C L E I N F O

Article history:
Received 27 March 2012
Received in revised form 2 July 2012
Accepted 26 July 2012
Available online 15 August 2012

Keywords:
Interpenetrating polymer, Coating,
Cross-linking agent, Heat resistance,
Impedance spectroscopy

A B S T R A C T

Polymer alloys, particularly interpenetrating polymer networks (IPNs) exhibit excellent coating properties. Often combination of polymers result in IPNs with controlled morphologies and synergistic behavior. In this study, corrosion-resistant IPNs were prepared from immiscible resins (epoxy, silicone and thiophene) using a cross-linking agent and a catalyst. GPC, FTIR, NMR, TG, DTA and SEM studies used to fix the best performing IPN. Surface morphology studies using SEM confirm the incorporation of silicone and polythiophene in to the epoxy polymer to form homogeneously micro structured IPN. The heat-resistance of the IPN was determined as per ASTM 2485. The improved corrosion resistance of the IPN was evaluated by AC impedance measurements.

1. Introduction

The search for polymers with desirable properties for a variety of applications is everlasting. In this context, interpenetrating polymer networks (IPNs), a class of polymer alloys exhibit a number of advantageous properties such as corrosion resistance, chemical resistance and improved mechanical characteristics. IPN may be described as a combination of chemically dissimilar polymers in which the chains of the polymers are completely entangled with one another, the entanglement being rendered permanent by homo-cross linking of polymeric chains. At least one of the constituent polymers is synthesized and/or cross-linked in the immediate presence of the other [1].

Most IPNs are classified under "compatibilized immiscible polymer blend alloys" [2]. In fact, two or more immiscible polymers are made compatible by special synthetic procedures to achieve fully compatibilized polymer alloys [3]. If only one polymer of the IPN is cross-linked while the other is in linear form, the system is termed as a semi-IPN. If all the member polymers are cross-linked, then the system is called a full-IPN [4]. This makes the field of application for IPN very wide and opens a floodgate for further developments. Since all the IPN is cross-linked they swell but do not dissolve in the presence of solvents and also exhibit suppressed creep and flow. The properties of the combined polymers depend on the properties of the member polymers and the way in which they are combined together [5,6]. IPN also help to improve the mechanical strength and elasticity of polymers [7,8] thus exhibits improved physical and chemical characteristics such as temperature sensitivity and interfacial compatibility [9,10]. IPN are newer variety of polymer hybrids with excellent physico-chemical properties [11].

Epoxy resin is well known for its chemical resistance and also useful as a maintenance coating [12,13]. The silicone resins are mainly used for protecting the metal surface from high temperature corrosion [14]. Dhoke et al. [15,16] reported the performance of epoxy–silicone, silicone–polypyrrole and silicone–polythiophene IPN for high temperature applications. Anandakumar and Sankaranarayanan [17] has reported the thermal properties of silicone based IPN.

In recent years, conducting polymers have been used as inhibitors for corrosion protection. The protective mechanism of conducting polymers is ascribed to the intelligent release of inhibitor anions, which is similar to Lira and Cordoba deTorresi [18] who studied the controlled release of medicine from IPN. However conducting polymers and pigments fail to protect large defective areas, although they offer excellent protection to small defect sites. Conducting polymer based IPN are widely used in actuators [19,20], but their use in protective coating is not well explained. Generally conducting forms of polypyrrole, polythiophene and polyaniline undergo property changes during reversible redox and pH switch reactions, properties include color, electrical conductivity, permeability, density and charge density. The presence of conducting polymer in the organic coating anodically protects the

---

[*] Corresponding author. Tel.: +91 4565 241367; fax: +91 4565 227779.
E-mail address: palrajsironmani@gmail.com (S. Palraj).

0300-9440/$ – see front matter © 2012 Elsevier B.V. All rights reserved.
http://dx.doi.org/10.1016/j.porgcoat.2012.07.014

base metal, by encouraging the formation of a passive oxide layer [21]. Characterization and evaluation of these IPN can lead to the formulation of an optimized IPN based system for the protection of steel substrates from corrosion as well as high temperature applications.

In this study, IPN was prepared by mixing different amounts of silicone resin with a constant amount of epoxy and thiophene monomers with other additives. The best performing IPN was identified, characterized with respect to heat resistant and corrosion properties were studied.

2. Materials and methods

2.1. Preparation of IPNS

Benzoyl peroxide (Qualigens, India) was dissolved in xylene (Qualigens, India), mixed with epoxy resin (CY 250, Ciba Geigy, Mumbai) and refluxed in a round-bottomed flask. A xylene solution of dibutyl tin laurate (Aldrich) and thiophene (E-Merck) was added drop wise to the refluxing mixture. After 90 min of refluxing silicone resin (Metro-ark) dissolved in xylene was added and refluxing was continued for 6 h. After refluxing, IPN was obtained by distilling off the excess solvent. The compositions of the four IPN thus prepared are given in Table 1.

2.2. Mechanism of formation of epoxy–polythiophene–silicone IPNs

The first step in the formation of IPN is the free radical formation, initiated by the benzoyl peroxide.

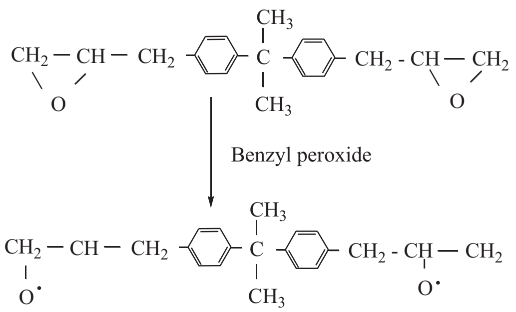

Once this highly reactive form of epoxy polymer is formed, thiophene readily penetrates and reacts with the methylene radical to form the corresponding thiophene polymer as given below:

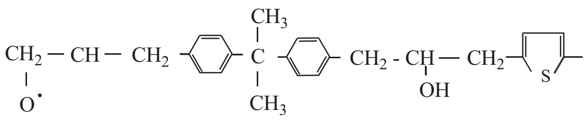

Thus formed IPN further reacts with the silicone polymer in the presence of the catalyst, dibutyl tin laurate to form higher molecular weight heat resistant IPN of the following structure.

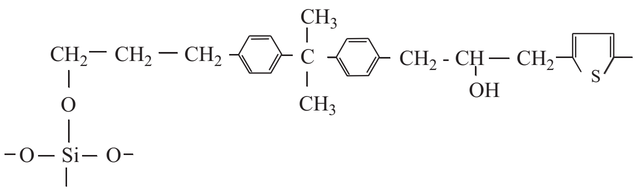

This high molecular weight IPN silicone polymer contains hydroxyl groups, which readily reacts with the curing agent (polyamide) to form a hard film over the substrate.

2.3. Characterization

The GPC analysis was carried out using software-controlled GPC of Jasco, Chromatopac. FTIR spectra were recorded using Paragon 500 FTIR spectrometer with a scan rate and resolution of 4 cm^{-1} and 64 at room temperature. Bruker 400 NMR spectrometer was utilized to record NMR spectrum. Thermal analytical studies were carried out using STA-1500 TG-DTA thermal station. Morphological studies were carried out using a Hitachi 3000-H scanning electron microscope. The coating thickness was measured using Minitest 600FN, EXACTO (range 0–2000 μm) coating film thickness meter. Gloss measurements of the coatings were carried out using Stargloss tester. Hate adhesion tester was used to determine the adhesion strength of the coatings. Impedance measurements were carried out using PARSTAT model 2273 electrochemical workstation. The electrochemical cell used for this study consists of epoxy–silicone–polythiophene coated steel as working electrode, a platinum foil as counter electrode and a saturated calomel electrode (SCE) as reference electrode and 3% NaCl as electrolyte. Impedance measurements were carried out periodically for different durations of time.

2.4. Coating preparation

The IPN were mixed with a hardener (polyamide, HY 840, Ciba Geigy) and applied over the pickled mild steel panels and dried at room temperature for 7 days. Four sets of panels of uniform thickness of S_1 (56.5 μm), S_2 (66 μm), S_3 (72.5 μm), and S_4 (76.5 μm) compositions were selected for gloss, adhesion and heat resistance and corrosion studies separately.

3. Results and discussion

3.1. Gloss measurements

The gloss measurements were carried out for 4 different IPNs incorporated coatings over mild steel to determine the best performing composition for further characterization. Fig. 1 shows the results of gloss measurement for the four compositions of IPN resins with hardener-coated over mild steel specimen. It indicates that except for sample S_2, the gloss characteristics improved with an increase in temperature up to 350 °C. For S_1, S_3 and S_4 it starts decreasing up to 380 °C whereas for S_2 the value remains constant beyond 270 °C. The indifferent behavior of S_2 is attributed to its homogenous nature of the composition. It is evident from the results that the silicone contents within the IPN alters the gloss properties of the coatings significantly at high temperatures. This is due to the fact that the homogeneity of the IPN is uniform and closely packed and agrees with Nayak et al. [22].

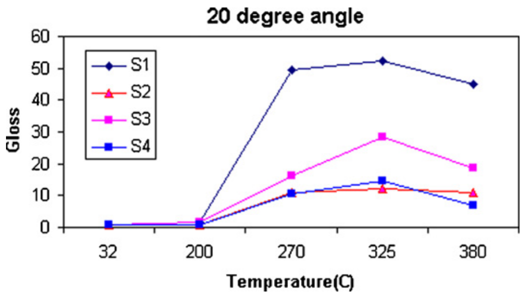

Fig. 1. Gloss measurement on IPN resin with hardener coated on mild steel.

Table 1
Compositions of the IPN resins.

Sample no	Silicone resin (mole)	Thiophene (mole)	Liquid epoxy (mole)	Benzoyl peroxide (mole)	Dibutyl tin laurate (mole)
1	0.00625	0.569	0.346	0.001	0.00259
2	0.01250	0.569	0.346	0.001	0.00259
3	0.01875	0.569	0.346	0.001	0.00259
4	0.0250	0.569	0.346	0.001	0.00259

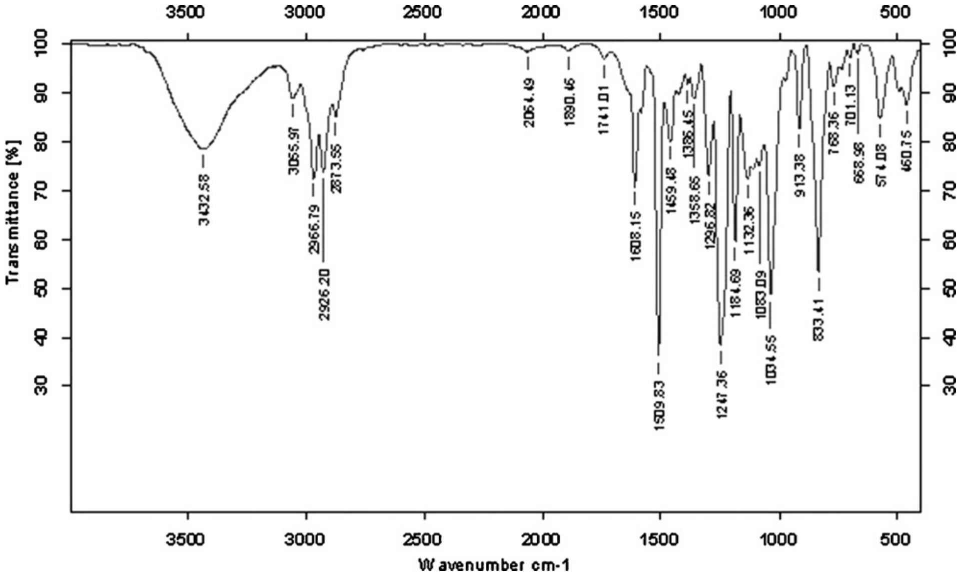

Fig. 2. FT-IR spectrum of the IPN resin coated on mild steel.

3.2. Adhesion and heat resistance properties

Table 2 shows the adhesion values measured for four different compositions of IPN resin with hardener coated on mild steel specimens. It is observed that the adhesion value of all the coatings increases steadily up to the temperature of 200 °C, remains almost equal up to 270 °C and with further increase in temperature the values decrease, the decrease being negligible in the case of S_2 composition. The decrease in the adhesion values of S_1, S_3 and S_4 are due to the initiation of the decomposition of coating at 270 °C and a total failure of the coating occurs beyond 350 °C.

Coated specimens were subjected to the heat treatment as per ASTM specification D2485. The experiment was conducted by exposing the coated samples to desired temperatures for different durations of time. The failure of the coating was observed visually by its color change, chalking, blistering, cracking and loss of adhesion. The coatings with S_1, S_3 and S_4 IPN failed beyond 350 °C; however the coatings with S_2 IPN were found to be intact even at 380 °C. These results establish the fact that when the silicone content (0.0125 mole) of the IPN is changed the adhesion and heat resistant properties of the coatings are affected. These results are also in good agreement with the gloss measurement studies. Hence the IPN (S_2) with an optimum content of silicone (0.0125 mole) was subjected to the further characterization individually as well as with polyamide for understanding the structure, thermal behavior and surface morphology.

Table 2
Adhesion properties.

Sample no	32 °C (Mpa)	200 °C (Mpa)	270 °C (Mpa)	325 °C (Mpa)	380 °C (Mpa)
S1	2.5	3.0	3.0	2.5	2.0
S2	4.5	5.0	5.0	4.8	4.7
S3	3.5	3.5	3.5	3.5	2.0
S4	2.5	3.5	3.0	2.5	1.8

3.3. IPN characterization

3.3.1. FT-IR spectrum

FTIR spectrum was recorded for the IPN (S_2) and IPN with hardener (polyamide) and they are shown in Figs. 2 and 3. The broad peak observed at 3432 cm^{-1} in Fig. 2 corresponds to the stretching vibration of the hydroxyl group. The peaks at 2926 cm^{-1} and 2873 cm^{-1} corresponds to $-CH_2-$ stretching vibration and the peaks at 2968 cm^{-1} and 3056 cm^{-1} to the methyl and $-CH$ attachments to aromatic rings. The peak at 1297 cm^{-1} confirms to the presence of aryl $-O-CH_2-$ group, while those at 1034 cm^{-1} and 1083 cm^{-1} are attributed to Si—O—Si and Si—O—C bonds in silicone, which are attached to the secondary carbon of the polymer network. The signal at 701 cm^{-1} indicates the presence of C—S stretching of thiophene, which agrees with Frederic Vidal et al. [23]. The $-C{=}C-$ stretching bonds of thiophene is indicated by the peak at 1510 cm^{-1} while the FTIR fingerprint of 2,5-disubstituted thiophene is indicated by the absorption peaks at 768 cm^{-1} and 833 cm^{-1}.

In Fig. 3, the peak at 1431 cm^{-1} is attributed to the presence of amide group. The broad band observed at 1610 cm^{-1} corresponds to the C=O group of polyamide. According to Kambour et al. [24], the peaks at 1511 cm^{-1} is indicative of a combination of C—N stretching and N—H bending of the groups attached to the secondary carbon of the polymer network. All the characteristic peaks of the IPN are also observed.

3.3.2. NMR spectroscopy

The ^{13}C and ^{1}H NMR studies of the IPN (S_2) were carried out to understand its structure are shown in Figs. 4 and 5. In the ^{13}C

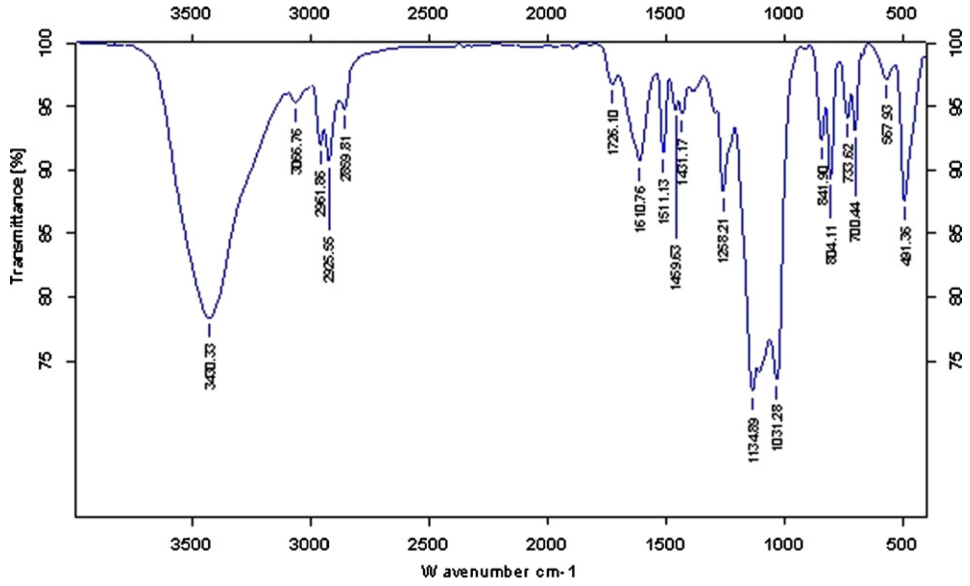

Fig. 3. FT-IR spectrum of the IPN resin with hardener coated on mild steel.

NMR spectrum (Fig. 4), the peak at 156.07 ppm confirms the presence of the aromatic ring attached to the —OCH$_2$ group. The peak at 143.37 ppm suggests the presence of 2,5-disubstitution in thiophene. The multiple peaks at 77 ppm correspond to the presence of the solvent. The signal at 113.74 ppm indicates that an aromatic carbon is attached to a quaternary carbon atom. The signals at 49.94, 44.48, 41.45 and 30.77 ppm are all due to different types of aliphatic carbons related to the —CH group attached with hydroxyl, methylene and methyl carbons in the main chain. The chemical shift at 68.4,49.9 and 44.4 ppm confirms the presence of epoxide groups [25–27].

The ^{1}H NMR spectrum of the IPN (S$_2$) is characterized by a signal at 7.27 ppm for the solvent (CDCl$_3$). The multiple peaks at 6.8 ppm correspond to the presence of proton in thiophene. The peaks at 7.1 and 7.2 confirm that there is a branching in the 2nd or 5th position of the thiophene ring, which agrees well with our earlier studies [28]. The corresponding proton signals at 1.651, 4.2–4.1 and 7.6–7.14 ppm correspond to the methylene group attached with thiophene, —OCH$_2$ group attached to the aromatic ring and the proton of the aromatic ring, respectively. The peaks at 2.9–2.7, 3.9–3.7 and 1.2 ppm correspond to the C—H group attached to hydroxyl, proton of the hydroxyl group

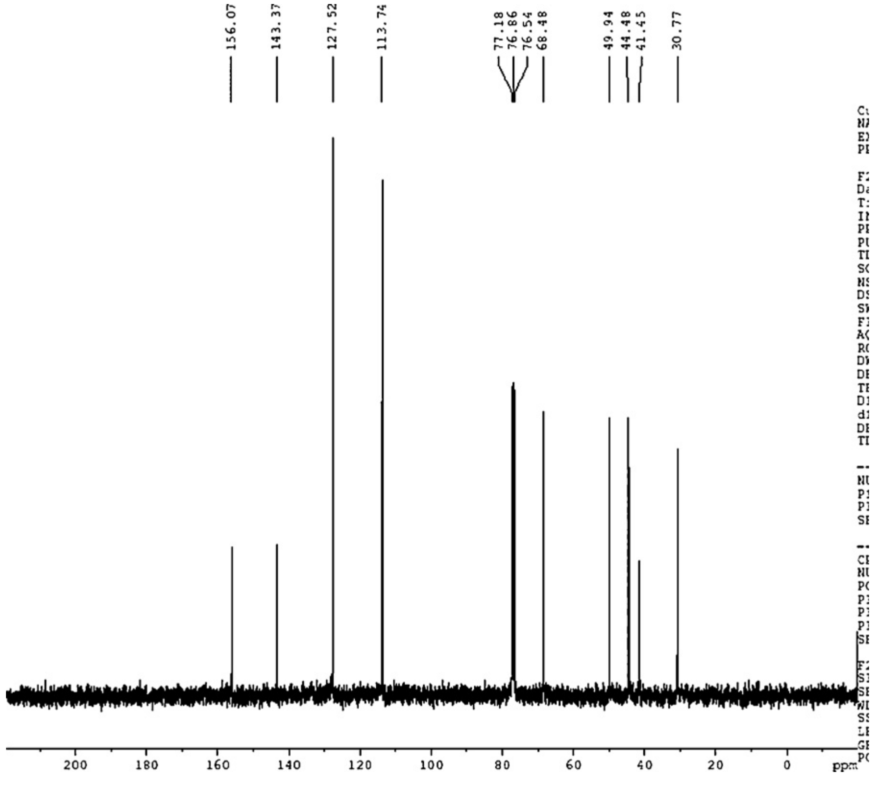

Fig. 4. ^{13}C NMR spectrum of the IPN resin.

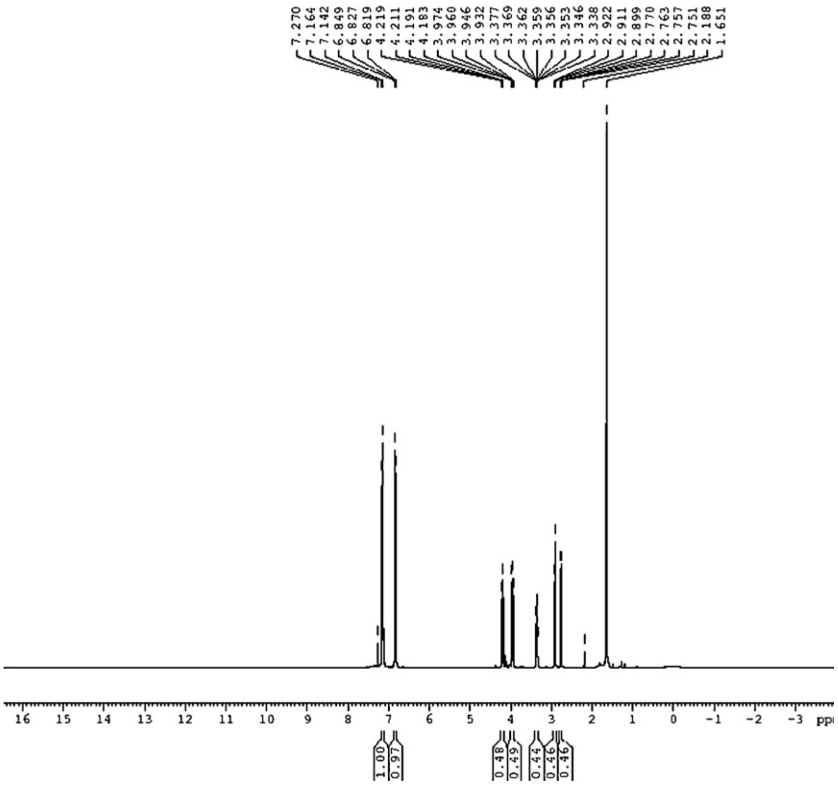

Fig. 5. ^{1}H NMR spectrum of the IPN resin.

and the methyl group of the proton attached with quaternary carbon.

3.3.3. Thermal analysis

Thermo gravimetric and differential scanning calorimetric analysis of the IPN was carried out at a heating rate 20 °C/min under flowing nitrogen atmosphere. Fig. 6 shows the thermal behavior of the epoxy–silicone–thiophene IPN. It shows that the decomposition/vaporization process commences around 150 °C with the weight loss reaching to 3.3% at 249 °C. This weight loss is due to the evaporation of superficial moisture and other volatile compounds present in the polymer. The weight loss registered up to 361 °C is 69%, indicates that beyond 250 °C the IPN resin is broke down possibly into two fragments, consequent to the loss of water and carbon

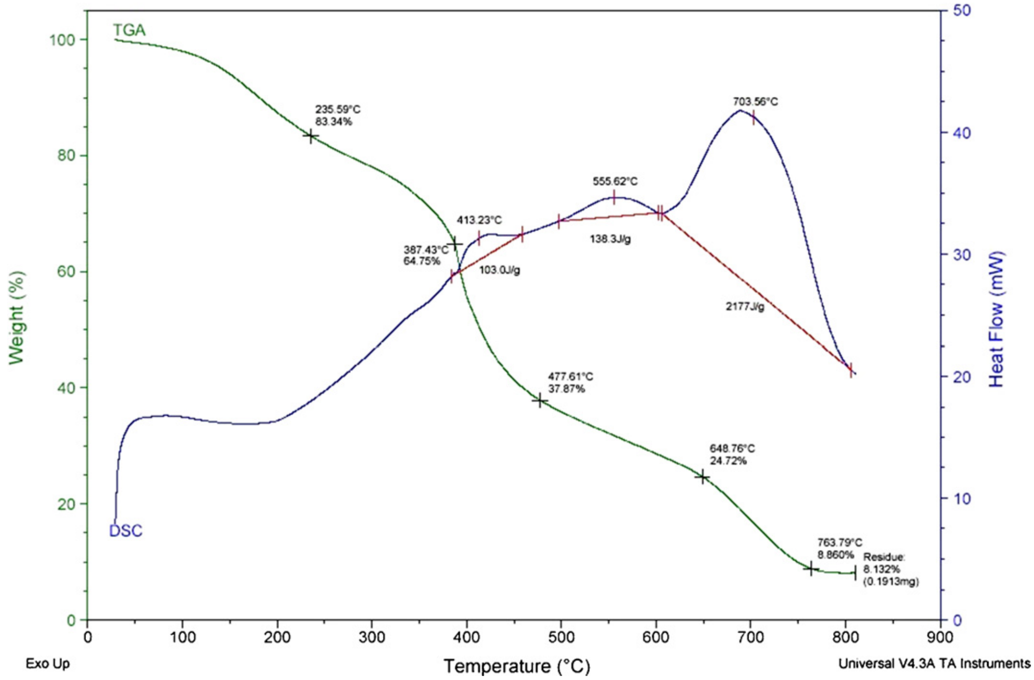

Fig. 6. TGA and DSC analysis of the IPN resin.

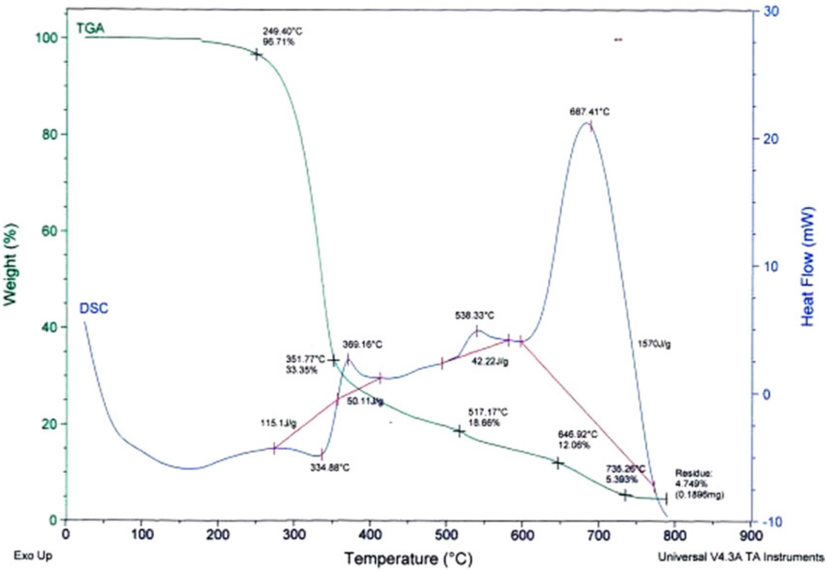

Fig. 7. TGA and DSC analysis of the IPN resin with hardener.

dioxide from the epoxy moiety. The silicone resin segment present in the IPN as well as the thiophene molecule appears to be stable up to 360 °C. Further fragmentation at 646.9 °C, with a weight loss of 19% is attributed to a breakdown of the bond between thiophene and silicone polymer. With a further increase in the temperature to 735 °C, the silicone polymer also fragments, yielding silica and oxygen. The weight of the residue remains at 5% of the original material at the end.

DSC gives information on the energy absorbed or liberated during the thermal treatment of the polymers. The differential thermal analysis of epoxy silicone IPN was reported in one of our previous studies [29]. This study indicated that two exothermic reactions occur between 250 and 350 °C and 350 and 400 °C. The exothermic reaction suggests that the formation of higher cross-linked polymer in the epoxy–silicone IPN. The second narrow band exothermic reactions are the dissociation of the IPN. The energy loss associated with patterns of epoxy silicone and thiophene indicate that, as the IPN decompose, an initial endotherm is followed by three exotherms. The endotherm peaks at 334.6 °C indicate absorption of 70.6 J/g of energy. The endothermic reactions also involve excess monomers (thiophene) present in the IPN structures. The peak at 368.7 °C with liberation of 50.5 J/g of energy is due to breaking of the bond between the bisphenol-A and thiophene. The second exothermic peak at 539 °C accompanied by liberation of 51.5 J/g of energy is related to breaking of the bond between thiophene and silicone; this process releases thiophene, which subsequently decomposes. These processes release sulfur dioxide and carbon dioxide, resulting in a stable silicone polymer. However, the silicone polymer also decomposes at 600 °C and complete disintegration of polymer occurs at 750 °C, leaving a residue of silica. The last of the decomposition process involves breakage of the strong —Si—O—Si— linkages within the polymer releasing an enormous quantity of energy (1541 J/g).

Fig. 7 shows the TGA and DSC profiles of a polyamide-cured IPN polymer. It is observed from the DSC pattern that glass transition in the IPN begins at 45 °C and reaches a steady state at 150 °C. Beyond 150 °C, degradation processes set in, proceeding up to 235.6 °C, where the weight loss reaches 16.6%. This loss in weight is mainly due to evaporation of superficial moisture and other volatile compounds present in the polymer as before. The weight loss recorded at 387 °C is about 35%. This indicates that the polyamide linkage present in the cured polymer is disbanded from the IPN and burned off from the coating. The IPN and the thiophene molecule are stable at this temperature. However, they fragment at 477.6 °C with the weight loss of 62%. This loss is due to breakdown of the bond between thiophene and the epoxy resin. Another weight loss of 75.3% observed at 648.8 °C is due to the breakdown of the bond between thiophene and the silicone resin. A further increase in temperature to 764 °C leads to fragmentation of the silicone polymer, yielding silica and oxygen as products with a final residual weight of 8%.

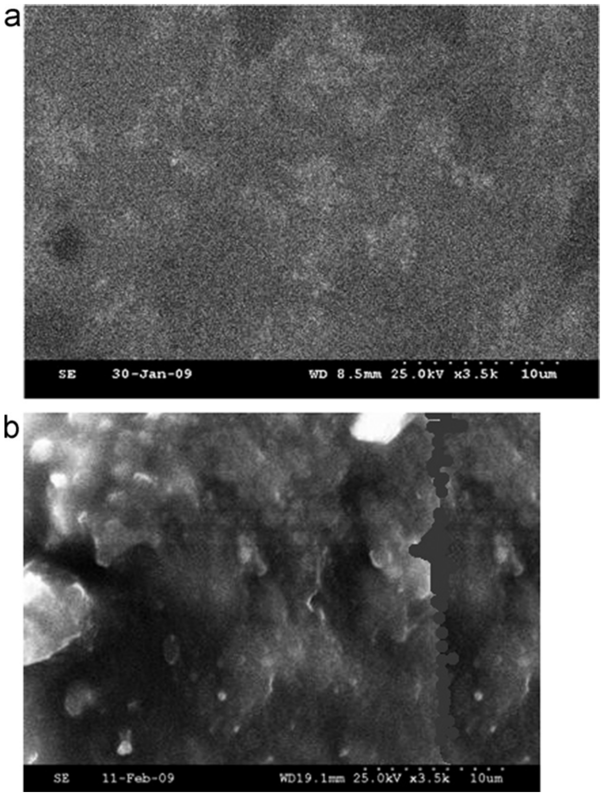

Fig. 8. (a) SEM micrograph of the IPN resin and (b) SEM micrograph of the IPN resin with hardener.

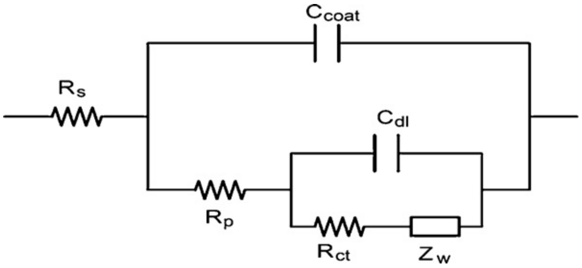

Fig. 9. Equivalent electrical circuit of coating system in aggressive environment.

The DSC profile of the IPN with the hardener shows an exothermic peak at 413.2 °C. The energy released in this step is 103 J/g, which corresponds to breaking of entanglement between the bisphenol-A and thiophene. A second exothermic peak at 555.6 °C, with 138.3 J/g of liberated energy is due to breaking of the bond between the thiophene and silicone moieties. This decomposition process is accompanied by liberation of sulfur dioxide and carbon dioxide, leaving behind a stable silicone polymer. However, the silicone polymer begins to degrade at about 610 °C and gets completely disintegrated at 800 °C, leaving a residue of silica. The cleavage of the strong —Si—O—Si— linkages in the polymer finally release an enormous quantity of energy (2177 J/g) during the decomposition process.

3.3.4. Morphology of IPN

The surface morphology of IPN as examined by SEM are shown in Fig. 8(a) and (b). The IPN is supposed to be cured uniformly in order to give a uniform final film. But in practice, nucleation of curing may initiate with different nucleation densities under different conditions. When the resin is subjected to curing/drying, nucleation is predominantly non-uniform, which leads to films with non-uniform thickness. It is seen from Fig. 8(a) that the silicone domains indicated by white globes, confirm the existence of the thiophene polymers in the IPN. The major portion covered by black region is indicative of epoxy resin dominating the IPN. This confirms that the thiophene monomers are incorporated with in the epoxy polymers to form interpenetrating polymer network. The non-uniformity vanishes when the hardener is added and dried. Fig. 8(b) shows a uniform morphology of the cured polymer with the existence of excess silicone domains. The increases in the black region indicate the formation of cross linkage between the IPN and the polyamide hardener. Hence the protective efficiency of these polymers enhances appreciably.

3.4. Electrochemical impedance measurements

Electrochemical impedance spectroscopy (EIS) was employed for the evaluation of the corrosion behavior of different IPN with hardener coated over mild steel in 3% NaCl. Fig. 9 represents the equivalent electrical circuit for the IPN-polyamide coated metal in aggressive corrosion environments, where R_S is the electrolyte resistance, R_P is the pore resistance of the coating, C_{coat} is the coating capacitance, R_{ct} is the charge transfer resistance, C_{dl} is the double layer capacitance and Z_W is the warburg impedance. The R_{ct} and C_{dl} for IPNs with hardener coated over mild steel immersed in 3% NaCl for 1, 24 and 168th hours of immersion are consolidated in Table 3.

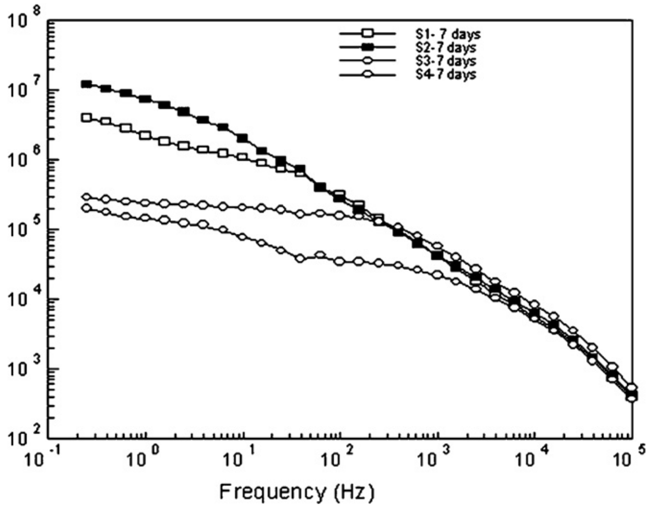

Fig. 10. Impedance behavior of IPN resin with hardener coated on mild steel in 3% NaCl.

The impedance plots showed that initially the coatings were capacitance in nature with very high resistance of $\cong 10^7$–10^8 Ω cm^2. Fig. 10 shows a Bode plot of the IPN resins with the hardener coated on mild steel in a 3% NaCl solution at the end of the 168th hour of immersion. The charge transfer resistance of S_1, S_3 and S_4 combinations in 3% NaCl decreases by 2–3 folds at the end of 168th hour of immersion and the double layer capacitance increases by an order of 1. However in the case of S_2-IPN incorporated coatings the changes in charge transfer resistance and double layer capacitance are less with little deviation from their initial values.

The values of the parameters related to the high frequency are C_{dl} and R_{ct}, which are considered to be coating properties changed with immersion time. Usually C_{dl} increases with the immersion time in the initial period and then remains approximately constant since the absorption of the water becomes saturated even if the immersion time further increases. Due to the porous nature of the coatings, formation of micro-cells occurs at the metal surface/coating interface. With the increase of immersion time and accumulation of corrosion products at the metal/coating interface, diffusion process was established. But in the case of S_2-IPN with polyamide, the structure of the cross-linked IPN-Polyamide contributed to the compactness of the coating which made water and chloride ions hard to transport and reduced the trend so that the corrosion resistance was improved. The EIS results also supports the fact that the IPNs with optimal silicone concentrations are comparatively less pore free with improved compactness. The content of absorbed water inside the coating as a measure of corrosion stability of a coating (from TG curves 4.2% to 2.8%), the lower value of the moisture content also indicate again the less porous structure which also contributes for a more stable system in a corrosive environment.

Table 3
The charge transfer resistance and double layer capacitance of IPN-polyamide coatings in 3% NaCl for different duration of time.

System with hardner	First hour		24th hours		168th hours	
	R_{ct} (Ω cm^2)	C_{dl} (F cm^{-2})	R_{ct} (Ω cm^2)	C_{dl} (F cm^{-2})	R_{ct} (Ω cm^2)	C_{dl} (F cm^{-2})
S1	3.25×10^8	7.5×10^{-10}	2.15×10^7	3.24×10^{-8}	4.01×10^6	9.9×10^{-8}
S2	2.51×10^7	1.5×10^{-10}	1.5×10^7	8.01×10^{-10}	1.32×10^7	9.10×10^{-10}
S3	5.24×10^7	2.06×10^{-10}	5.0×10^6	9.2×10^{-9}	3.14×10^5	4.05×10^{-9}
S4	1.45×10^8	6.55×10^{-10}	3.5×10^7	3.5×10^{-9}	2.64×10^5	5.5×10^{-9}

4. Conclusion

Based on the investigations together with NMR and FT-IR data confirm the presence of epoxy, thiophene and silicone linkages in the prepared IPN resin. The morphology of IPN also confirms the interpenetration of the polymers. Gloss and adhesion measurements reveal that adhesion improved with an increase in temperature. However, a further increase in the temperature leads to deterioration of the adhesion. TG-DTA studies suggest that there is improvement in heat resistance properties of the modified IPN. The heat resistance property of the IPN shows an upper stability limit of 380 °C for IPN with optimum silicone content and to 325 °C for IPN with higher silicone content. Impedance measurements show that IPN (S_2) exhibits better corrosion resistances when compared to other samples.

Acknowledgment

The authors wish to express their sincere thanks to The Director, CSIR-CECRI for his kind permission to publish this work.

References

[1] L.H. Sperling, Source-based Nomenclature for Polymer Blends, IPN and Related Materials, Division of Polymer Chemistry Nomenclature Committee Document, 1984.
[2] Y.S. Lipatov, A.Y. Nesterov, T.D. Ignatova, N.P. Gudima, D.T. Gritseriko, Eur. Polym. J. 22 (1986) 86.
[3] D. Klempner, H.L. Frisch, J. Polym. Sci. 8 (1970) 921.
[4] X. Hou, K.S. Siow, Polymer 42 (2001) 4181.
[5] P.F. Bruins, Polymer Blends and Composites, Wiley Interscience, NY, 1970.
[6] L.H. Sperling, Interpenetrating Polymer Networks Advances in Chemistry, American Chemical Society, Washington, D.C., 1994.
[7] N. Nemirovski, M.S. Silverstein, M. Narkis, Polym. Adv. Technol. 7 (1996) 247.
[8] K.C. Frisch, D. klempner, S. Migdal, Polym. Eng. Sci. 14 (1974) 76.
[9] Tomko, US Patent No. 6166127, December 26, 2000.
[10] B. Suthar, M. Dave, K. Jadav, J. Appl. Polym. Sci. 50 (1993) 2143.
[11] Lee, Takayuki Kawamura, E.F. Stevens, US Patent No. 4569964, February 11, 1986.
[12] Surface Coating Association of Australia, Surface Coatings, vol. 1, Chapman and Hall, London, 1993.
[13] S.M. Krishnan, P.S. Mohan, J. Coat. Technol. Res. 5 (2008) 131.
[14] C.H.Hare, Paint India, XL VIII (2) (1998) 35.
[15] Shailesh K. Dhoke, S. Palraj, K. Maruthan, M. Selvaraj, Prog. Org. Coat. 56 (2006) 53.
[16] Shailesh K. Dhoke, S. Palraj, K. Maruthan, M. Selvaraj, Prog. Org. Coat. 59 (2007) 21.
[17] S. Anandakumar, T.S.N. Sankaranarayanan, Prog. Org. Coat. 45 (2002) 323.
[18] Luiz M. Lira, Susana I. Cordoba deTorresi, Electrochem. Commun. 7 (2005) 717.
[19] Rohwerder Michael, Michalic Adam, Electrochim. Acta 53 (2007) 1300.
[20] Cedricpherre, Frederic Videl, Myacinthe Randriamahazaka, Dominique Teyssie, Clanechevrst, Polymer 46 (2005) 7771.
[21] J.N. Barisci, T.W. Lewis, G.M. Spinks, C.O. Too, G.G. Wallace, J. Intell. Mater. Syst. Struct. 9 (1998) 723.
[22] P.L. Nayak, S. Lenka, S.K.Panda, T. Pattniak, J. Appl. Polym. Sci. 47 (1993) 1089.
[23] Frederic Vidal, Cedric Plesse, Guillaume Palaprat, Abderrahmane, Kheddar, Johnciterin, Dominique Teyssie, Claude Chevrot, Synthetic Met. 156 (2006) 1299.
[24] R.P. Kambour, H.J. Klopfer, J. Appl. Polym. Sci. 26 (1981) 847.
[25] Charles J. Pouchert, The Aldrich library of IR Spectra, Aldrich Chemical Company INC, 940W St. PaulAve, Milwaykee, Wisconsin 53233.
[26] D.J. Liaw, Polymer 38 (1997) 5217.
[27] C.S. Wu, Y.L.Liu, Y.S. Chiu, Polymer 43 (2002) 4277.
[28] Soo-jin Park, Fan-Long Jin, Jae-Rock Lee, Macromole. Res. 13 (2005) 8.
[29] A.M. Kamalan Kirubakaran, S. Palraj, M. Selvaraj, G. Rajagopal, J. Appl. Polym. Sci. 119 (2010) 2339.